Scaling of Haversian Canal Surface Area to Secondary Osteon Bone Volume in Ribs and Limb Bones

John G. Skedros,[1]* Alex N. Knight,[1] Gunnar C. Clark,[1] Christian M. Crowder,[2] Victoria M. Dominguez,[3] Shijing Qiu,[4] Dawn M. Mulhern,[5] Seth W. Donahue,[6] Björn Busse,[7] Brannon I. Hulsey,[8] Marco Zedda,[9] and Scott M. Sorenson[1]

[1]*Department of Veterans Affairs Medical Center, Bone and Joint Research Laboratory, Salt Lake City, UT*
[2]*Office of the Armed Forces Medical Examiner, Armed Forces Medical Examiner System, Dover AFB, DE*
[3]*Division of Anatomy, The Ohio State University, Columbus, OH*
[4]*Bone and Mineral Research Laboratory, Henry Ford Hospital, Detroit, MI*
[5]*Department of Anthropology, Fort Lewis College, Durango, CO*
[6]*Department of Mechanical Engineering, Colorado State University, Fort Collins, CO*
[7]*Department of Osteology and Biomechanics (IOBM), University Medical Center Hamburg-Eppendorf, Hamburg, Germany*
[8]*Department of Anthropology, University of Tennessee, Knoxville, TN*
[9]*Department of Animal Biology, University of Sassari, Sassari, Italy*

KEY WORDS bone remodeling; bone adaptation; bone metabolism; calcium exchange

ABSTRACT Studies of secondary osteons in ribs have provided a great deal of what is known about remodeling dynamics. Compared with limb bones, ribs are metabolically more active and sensitive to hormonal changes, and receive frequent low-strain loading. Optimization for calcium exchange in rib osteons might be achieved without incurring a significant reduction in safety factor by disproportionally increasing central canal size with increased osteon size (positive allometry). By contrast, greater mechanical loads on limb bones might favor reducing deleterious consequences of intracortical porosity by decreasing osteon canal size with increased osteon size (negative allometry). Evidence of this metabolic/mechanical dichotomy between ribs and limb bones was sought by examining relationships between Haversian canal surface area (BS, osteon Haversian canal perimeter, HC.Pm) and bone volume (BV, osteonal wall area, B.Ar) in a broad size range of mature (quiescent) osteons from adult human limb bones and ribs (modern and medieval) and various adult and subadult non-human limb bones and ribs. Reduced major axis (RMA) and least-squares (LS) regressions of HC.Pm/B.Ar data show that rib and limb osteons cannot be distinguished by dimensional allometry of these parameters. Although four of the five rib groups showed positive allometry in terms of the RMA slopes, nearly 50% of the adult limb bone groups also showed positive allometry when negative allometry was expected. Consequently, our results fail to provide clear evidence that BS/BV scaling reflects a rib versus limb bone dichotomy whereby calcium exchange might be preferentially enhanced in rib osteons. Am J Phys Anthropol 151:230–244, 2013.

In many mammalian species, bones of the appendicular skeleton achieve and maintain adequate tissue mechanical properties through the process of remodeling, which is mediated by the formation of secondary osteons (Haversian systems) (Currey, 2002; Lieberman et al., 2003; Martin, 2003). These osteons are formed by basic multicellular units (BMUs) that include the actions of osteoclasts and osteoblasts. In the perspective of the interplay between these functional units and bone organ homeostasis, parallels have been drawn between basic functional units in other organ systems; for example, nephron units and kidneys (Frost, 2003). To some investigators, this analogy may seem appropriate when osteons are viewed as metabolic entities that principally function to maintain calcium balance. This analogy, however, seems less appropriate when osteons are viewed as mechanical entities—with relatively greater importance being placed on their role in attenuating the growth and/or accumulation of microdamage (Martin et al., 1998; Currey, 2002; Skedros et al., 2011b). In view of this metabolic/mechanical dichotomy, much remains to be learned about how the relative importance of these different osteon functions might be at work in specific bone types, where metabolic functions might predominate over mechanical functions (e.g., ribs vs. weight-bearing bones, respectively) (Raab et al., 1991; Tommerup et al., 1993; Robling and Stout, 2003; Pfeiffer et al., 2006). This is an important consideration because anthropological studies

Grant sponsors: U.S.A. Department of Veterans Affairs medical research funds and Orthopaedic Research and Education Foundation (OREF; medical research fund); Grant number: 01-024; Grant sponsor: NIH; Grant numbers: DK43858 and AR050420; Grant sponsor: The Graduate School at the University of Colorado at Boulder; Grant sponsor: The German Research Foundation (DFG)/University Medical Center Hamburg-Eppendorf; Grant number: BU 2562/2-1; Grant sponsor: The University of Tennessee William M. Bass Endowment.

*Correspondence to: John G. Skedros, 5323 South Woodrow Street, Suite 200, Salt Lake City, Utah, USA 84107. E-mail: jskedrosmd@uosmd.com

Received 30 May 2012; accepted 6 March 2013

DOI: 10.1002/ajpa.22270
Published online 30 April 2013 in Wiley Online Library (wileyonlinelibrary.com).

of secondary osteons in ribs have provided a great deal of what is now known about osteonal remodeling dynamics in general. However, it is unclear to what extent the physiological functions of rib osteons can be generalized to osteons that are found in limb bones.

As a working hypothesis, we expected differences in scaling relationships of osteon bone surface versus bone volume that differentiate ribs and limb bones because of their notably different mechanical, physiologic, and metabolic functions. This hypothesis is based on data showing that ribs and limb bones can be distinguished by their different: 1) morphogenetic field development, 2) metabolic activities, which correlate with different basal, stress, and/or hormone induced bone remodeling rates, 3) mechanosensitivity, and 4) habitual loading frequency and strain magnitudes. For example, during development the majority of a mammalian rib develops from the sclerotomes of the somites, in contrast to limb bones, which arise from lateral plate mesoderm (Huang et al., 2000; Hall, 2005). Ribs are phylogenetically primitive, appearing as elements of the axial skeleton in the fossil record well before limb bones, likely enabling differential evolution in physiology (Shearman and Burke, 2009; Schilling, 2011). Ribs are also metabolically more active and sensitive to hormonal fluctuations and changes such as occurs during lactation and metabolic stress (Banks et al., 1968; Hillman et al., 1973; Wilson et al., 1998; Baxter et al., 1999; Ott et al., 1999; Vajda et al., 1999), but less responsive than limb bones to increased exercise-related loading (Raab et al., 1991; Tommerup et al., 1993). Basal bone remodeling rates are relatively greater in ribs than in limb bones of the same animal (Amprino and Marotti, 1964; Wilson et al., 1998; Vajda et al., 1999; Mulhern, 2000; Skedros et al., 2003), and there are significant differences in mechanosensitivity between osteocytes/osteoblasts of the axial versus appendicular skeleton (Raab et al., 1991; Tommerup et al., 1993; Rawlinson et al., 1995; Vatsa et al., 2008). Finally, ribs receive frequent, usually stereotypical (Bellemare et al., 2003), and often low-strain loading (at least in humans); for example, during respiratory movements even when the animal is recumbent (Jordanoglou, 1969; Andriacchi et al., 1974; Crowder and Rosella, 2007; Cagle, 2011).

As an initial step in investigating the metabolic/mechanical dichotomy that may exist between osteons of ribs and limb bones, we explored simple scaling relationships between the area of the bone surface (BS) of osteon central canals (Haversian canals) and bone volumes (BV) of osteon walls. In two dimensions (2D), Haversian canal surface area scales as perimeter (length, l; or HC.Pm) and the osteon wall volume scales as area (l^2; or B.Ar).[1] We tested the hypothesis that HC.Pm/B.Ar (BS/BV) scaling relationships in fully formed (i.e., mature) osteons of rib bones would exhibit positive allometry in order to keep osteon central canal size (HC.Pm) large enough for: 1) efficient calcium exchange from the osteon wall (B.Ar) to the systemic circulation (Qiu et al., 2003; Qiu et al., 2010), and 2) to avoid placing some osteocytes at risk of ischemia (Ham, 1952; Martin, 2000; Metz et al., 2003) (Fig. 1). However, increasing the size of Haversian canals could result in deleterious strength reductions as the result of the increased porosity (Donahue and Galley, 2006). Avoiding this is especially important in the limb bones where peak strain magnitudes are probably habitually greater than in ribs, and where regional heterogeneity in osteon size (diameter) is likely mechanically beneficial (Hiller et al., 2003; van Oers et al., 2008; Skedros et al., 2013). In this perspective we predicted negative HC.Pm/B.Ar allometry in osteons of limb bones. Hence, HC.Pm/B.Ar in limb-bone osteons will increase at a comparatively lower rate with respect to absolute increases in osteon size (i.e., osteonal porosity will remain relatively low in limb bone osteons; Fig. 1). In general, these predictions are based on the pervasive view that convective nutrient delivery and calcium exchange to and from osteocytes across the Haversian canal surface will be optimized differently in ribs versus limb bones primarily because mechanical requirements outweigh metabolic demands in the appendicular skeleton (Parfitt, 1983; Tommerup et al., 1993; Robling and Stout, 2003; Pfeiffer et al., 2006).

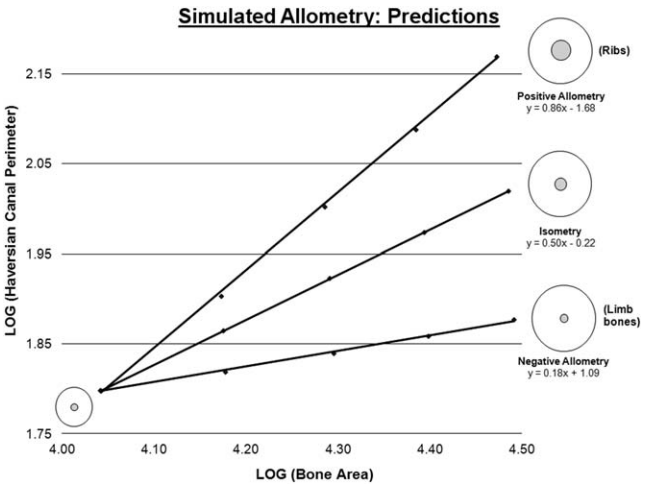

Fig. 1. Regression plots showing three predicted osteon Haversian canal surface area (BS or HC.Pm) to osteon bone volume (BV or B.Ar) relationships. The top regression line illustrates the positive allometry predicted in rib osteons. The middle regression line illustrates isometric scaling, which was not predicted to occur in any of the bones. The bottom regression line illustrates the negative allometry predicted in limb bone osteons. The data used for these graphics included HC.Pm measured in mm and B.Ar measured in mm^2.

MATERIALS AND METHODS

Using light or electron microscopy, images were obtained from human ribs (Mulhern, 2000; Qiu et al., 2003; Crowder, 2005), femora (Kerley, 1965; Ericksen, 1991; Busse et al., 2010a,b; Skedros et al., 2012), and metatarsals (Donahue et al., 2000), in addition to non-human ribs (deer and dog) (Morris, 2007; Dominguez and Crowder, 2012) and limb bones. The non-human limb bones include calcanei (sheep, deer, elk, and horse) (Skedros et al., 2011a), radii (horse) (Skedros et al., 2011a), humeri (deer and dog) (Morris, 2007; Dominguez and Crowder, 2012), femora (deer, cow, horse, dog, and black bear) (Morris, 2007; Zedda et al., 2008; Dominguez and Crowder, 2012; Gray et al., 2012), metacarpals (black bear and horse) (Hulsey et al., 2009; Skedros et al., 2011a), and metatarsals (black bear) (Hulsey et al., 2009). The skeletal maturity, specimen preparation, and histomorphometric methods used to obtain and analyze the digitized images of complete and fully formed secondary osteons from these bones are summarized in Table 1. Slides from Morris (2007), Kerley (1965),

[1]For the purposes of this study, osteon BS is expressed as HC.Pm and osteon BV is expressed as B.Ar. The rationale for this is described in the Methods section.

TABLE 1. Specimens, tissue processing, and microscope imaging methods

Authors and references	Specimen	No. specimens	Skeletal maturity	Male/female	Location of specimen in the bone	Thickness of specimen for imaging	Embedment	Magnification	Type of imaging
Skedros et al. (2012)	Human Femur (JS)	12	Mature	2M/10F	Proximal shaft	100 μm	PMMA	50×	PL
Skedros et al. (2011a)	Sheep Calcaneus (*O. aries*)	7	Mature	Female	Midshaft	5 mm	PMMA	50×	BSEI
Skedros et al. (2011a)	Deer Calcaneus (*O. hemionus*)	10	Mature	Male	Midshaft	5 mm	PMMA	50×	BSEI
Skedros et al. (2011a)	Elk Calcaneus (*C. elaphus*)	7	Mature	Male	Midshaft	5 mm	PMMA	50×	BSEI
Skedros et al. (2011a)	Horse Calcaneus	7	Mature	Mixed	Midshaft	5 mm	PMMA	50×	BSEI
Skedros et al. (2011a)	Horse Radius	10	Mature	Mixed	Midshaft	5 mm	PMMA	50×	BSEI
Skedros et al. (2011a)	Horse Metacarpal	9	Mature	Mixed	Midshaft	5 mm	PMMA	50×	BSEI
Crowder (2005)	Human Rib[a] (Spitalfields)	223	Mature	108M/112F/ 3 unknown	Midsternal (unknown rib)	50–80 μm	Epoxy	100×	PL
	Human Femur (CC)+	213	Mixed	105M/108F	Midshaft	50–80 μm	None	40×	PL
Dominguez and Crowder (2012)	Deer Rib[b] (*O. virginianus*)	6	Mixed	Unknown	Midshaft	100–300 μm	Epoxy	40×	Light
Morris (2007)	Deer Humerus	5	Mixed	Unknown	Midshaft	100–300 μm	Epoxy	40×	Light
Morris (2007)	Deer Femur	4	Mature	Unknown	Midshaft	100–300 μm	Epoxy	40×	Light
Morris (2007)	Dog Rib	6	Mature	Unknown	Midshaft	100–300 μm	Epoxy	40×	Light
Morris (2007)	Dog Humerus	6	Mature	Unknown	Midshaft	100–300 μm	Epoxy	40×	Light
Morris (2007)	Dog Femur	6	Mature	Unknown	Midshaft	100–300 μm	Epoxy	40×	Light
Qiu et al. (2003)	Human Rib (Modern)	9	Mature	Male	Mid 1/3 (5th, 6th, 7th rib)	50 μm	None	10×	Light
Mulhern (2000)	Human Rib (Nubian)[a]	80	Mixed	35M/45F	Mid 1/3 (6th rib)	40 μm	Epoxy	100×	Light
Donahue et al. (2000)	Human Metatarsal	15	Mature	8M/7F	Midshaft (2nd, 5th MTs)	120 μm	PMMA	23×	Light
Gray et al. (2012)	Black Bear Femur[a] (*U. americanus*)	47	Mixed	Mixed	Midshaft	70–90 μm	PMMA	40×	Light
Busse et al. (2010a,b)	Human Femur (BB)	26	Mixed	Mixed	Proximal Shaft	20 μm	PMMA	80×	Light
Hulsey et al. (2009)	Black Bear Metacarpal[a] (*U. americanus*)	7	Mixed	Unknown	Midshaft (2nd MCs)	150 μm	Epoxy	10×	Light
Hulsey et al. (2009)	Black Bear Metatarsal[a]	9	Mixed	Unknown	Midshaft (2nd MTs)	150 μm	Epoxy	10×	Light
Zedda et al. (2008)	Cow Femur[a]	20	Mature	Mixed	Midshaft	50 μm	None	4×, 10×	Light
Zedda et al. (2008)	Horse Femur[a]	20	Mature	Mixed	Midshaft	50 μm	None	4×, 10×	Light

[a] Haversian canal perimeter was calculated.
[b] The majority of the deer rib sample was skeletally immature, but all osteons measured were fully formed.
M = Male; F = female; PMMA = polymethyl methacrylate; PL = polarized light; BSEI = backscattered electron imaging; JS = John Skedros; CC = Christian Crowder; BB = Björn Busse; + = human femora from Kerley (1965) sample, Ericksen (1991) sample, and New York City Office of Chief Medical Examiner (NYC-OCME) Forensic Anthropology Unit (obtained by C. Crowder); MTs = metatarsals; MCs = metacarpals. The deer from Morris (2007) are *O. virginianus*.

and Ericksen (1991) were re-analyzed for the present study. Some of the deer samples included immature animals, which are designated as "sub-adults" because they were within one year of skeletal maturity (written communication, Zoe Morris, March 2012). The black bear samples were separated as immature (≤5 years old) and mature (≥6 years old). These bones were included in order to determine if the osteonal HC.Pm/B.Ar (BS/BV) analysis might be influenced when fully formed osteons are obtained from animals that are still growing.

Mature osteons were selected, and the criteria for this selection included the lack of poorly mineralized (i.e., younger) bone (BSE images) or osteoid (light microscopy) (Skedros et al., 2011a). The osteons were also examined to ensure that the margins of the Haversian canals did not appear to have regional staining variations (light microscopy) or regional mineralization variations (BSE images) that are inconsistent with a resting surface (Skedros et al., 2005). The osteons that were quantified were typically quasi circular with shape factors greater than 0.8 (1.0 = perfect circle). However, some of the investigators did not make this measurement, but confirmed that atypical osteons, as described by Skedros et al. (2007), were excluded from their analysis. Using digitized images, the outer perimeter (cement line) of each complete/mature osteon was traced using the following image analysis programs: 1) most authors used NIH Image, U.S. National Institutes of Health; available at: http://rsb.info.nih.gov/nih-image/, 2) Donahue used BIOQUANT OSTEO, Nashville, Tennessee, USA, and 3) Hulsey used Image-Pro Express, version 4.5.1.3, Media Cybernetics, Inc., Silver Spring, Maryland, USA. The osteon area (On.Ar) was then determined. The perimeter of each Haversian (central) canal (HC.Pm) was also traced and the area (HC.Ar) was then determined. Assuming that the Haversian canal was circular, the HC.Pm was calculated for some of the bone samples from HC.Ar (see asterisks in Table 1; in some cases the HC.Pm was directly measured). Osteon bone area (B.Ar) was calculated as On.Ar minus HC.Ar.

Allometric analyses of relationships of bone surface (HC.Pm) and bone volume (B.Ar)

For the regression analyses, the following parameters were used: osteon area (On.Ar), osteon diameter (On.Dm), osteon bone area (B.Ar), and Haversian canal perimeter (HC.Pm), diameter (HC.Dm), and area (HC.Ar). According to the ASBMR Histomorphometry Nomenclature Committee (Parfitt et al., 1987), the two-dimensional (2D) parameters of HC.Pm and B.Ar in osteons can be expressed in three-dimensional (3D) parameters as bone surface and bone volume, respectively. Thus HC.Pm/B.Ar can be regarded as the bone surface to bone volume (BS/BV) ratio (Qiu et al., 2003). For the purposes of this study, BS/BV is expressed as HC.Pm/B.Ar. The rationale for using these expressions, rather than Haversian canal and osteon wall areas, is that HC.Pm and B.Ar more closely correspond to the actual surface and volume involved in the dynamics of trans-canal and trans-osteonal nutrient and molecular transport and exchange. The use of HC.Pm and B.Ar also provide data in a fashion that will facilitate comparisons with future studies where high resolution micro-computed tomography will be used to analyze BS and BV of entire osteons (discussed further below).

Allometric scaling relationships between HC.Pm and B.Ar for all osteons in each species, and within specific regions within some non-human limb bones, were examined using the exponential equation (Huxley and Tessier, 1936; Schmidt-Nielsen, 1984):

$$y = a \cdot \mathrm{x}^{\mathrm{b}}$$

This was log-transformed in order to convert it to a linear function:

$$\log(y) = \log(a) + (b)\log \cdot x$$

In this equation, **log a** represents the y intercept, and the exponent ***b*** represents the slope of the best-fit line that was obtained using least-squares and reduced major axis (RMA) regression analyses, as described below (Schmidt-Nielsen, 1984; Swartz and Biewener, 1992). The $\log_{10}$-transformed HC.Pm (BS) data were plotted on the *y*-axis (ordinate), and the $\log_{10}$-transformed B.Ar (BV) data were plotted on the *x*-axis (abscissa). This regression analysis yielded the linear slope of the HC.Pm/B.Ar relationship. In the context of conventional scaling analyses (Schmidt-Nielsen, 1984), isometry is seen when the proportionality in logged HC.Pm/B.Ar data scale with a slope of 0.5 (i.e., 1:2). In contrast, a slope of <0.5 represents negative allometry, and a slope of >0.5 represents positive allometry (Fig. 1). We considered a slope to be negatively or positively allometric if the 95% confidence interval surrounding the slope did not contain 0.5.

Allometric relationships of the osteons were assessed for some non-human limb bones (sheep, deer, elk, and equine calcanei, and equine radii) in the contexts of habitual regional strain modes (tension, compression) and magnitudes (highest in "compression" regions), and osteonal remodeling rates (highest in plantar "tension" cortices of the calcanei) (Mason et al., 1995; Su et al., 1999; Skedros et al., 2011c). Additionally, the collagen/lamellar organization of the osteons ("osteon morphotypes") in these regions differ as adaptations for these strain mode differences (Skedros et al., 2009; Skedros, 2012). If differences in "osteon morphotypes" affect the efficiency of calcium exchange across quiescent HC surfaces (perhaps because of differences in their lacunar-canalicular geometries (Mishra and Knothe Tate, 2003; Kerschnitzki et al., 2011)), then a difference in HC.Pm/B.Ar scaling might be detected between these morphotypes. We also expected that while HC.Pm/B.Ar relationships would generally show negative allometry in limb bones when compared with ribs, this relationship would be more strongly negative in the more highly strained "compression" regions. In contrast, because the plantar cortices of these bones exhibit increased remodeling rates suggesting increased metabolism, it was anticipated that proportionally larger canals would be seen in the fully formed osteons in these regions.

Ordinary least squares regression models assume that all observations, or measurements on osteons, are independent, which would be the case if one osteon per bone specimen was used. Our data represented nested (clustered) data, with measurements made on multiple osteons from the same bone specimen. In nested data, the osteons from the same bone specimen are more alike than they are between bone specimens, and so the measurements made on the osteons are not all independent. To account for this lack of independence, mixed effects linear regression models were used (also known as multi-level models) (Stata 12.1 software, StataCorp, College Station, TX). Mixed effects models provide correct standard errors, and hence correct *P* values and confidence intervals; whereas,

ordinary models under-estimate the standard error, producing P values that are too small and confidence intervals that are too narrow.

Another advocated approach for allometric data is reduced major axis (RMA) regression. RMA regression is proposed as preferable in the contexts of: 1) correlations that are moderate or strong ($r > 0.5$), 2) there is potential error in both the dependent and independent variables, and 3) the variables modeled, HC.Pm and B.Ar in this study, do not naturally correspond to the usual dependent and independent variable sense, where one depends on or is a function of the other (Smith, 2009). The RMA model, however, can yield erroneous results in bivariate comparisons with low correlations (Seim and Saether, 1983; Swartz and Biewener, 1992).

We fitted both mixed effects models and RMA models to our data. However, the software used for the RMA models (PAST Version 2.16, Øyvind Hammer, University of Oslo, 2012) (Hammer et al., 2001) could not account for nesting/clustering of osteons within bone specimens, instead requiring the use of all individual osteon measurements, thus violating the assumption of independence. Although the proposed advantage of RMA is its ability to fit a line to a bivariate relationship when there are no conventional dependent and independent variables, the way it is computed posed a problem because the software is not designed for nested data. Because RMA is currently not an appropriate statistical test for nested data, RMA slopes, correlation coefficients, P values, and 95% confidence intervals are provided for only the un-nested data (i.e., considering all osteons as independent observations). The 95% confidence intervals for the RMA slopes were obtained using a bootstrapping method (Hofman, 1988; Plotnick, 1989). In the context of the least-squares analyses, the slopes, or effect estimates, were nearly identical in both the linear and mixed effects models, but differed in P values and confidence intervals. Therefore, least-squares slopes, correlation coefficients, P values, and 95% confidence intervals are provided for the nested and un-nested data. Providing these nested and un-nested data allow for the consideration of the HC.Pm/B.Ar relationships in some bones that might seem less clear when evaluated in terms of only the nested data (e.g., human metatarsals and equine radii).

In the mixed effects model as well as the RMA and least-squared models, $\log_{10}$-transformations were used to make the relationship more linear, thus providing a better model fit. That is, both the outcome variable (HC.Pm) and the predictor variable (B.Ar) were first transformed to $\log_{10}$ measurements, which resulted in fitting the data to the "allometric" function $y = 10^b x^a$, where the b is the slope and a is the y-intercept (Hammer et al., 2001). When both the outcome and predictor variables are $\log_{10}$-transformed, applying the following formula to the slope, $100(10^{B\log_{10}(1.01)} - 1)$, where B is the regression slope, the slope can be interpreted as the percentage increase in the average value of the outcome for each 1% increase in the predictor (Vittinghoff et al., 2005). However, the formula only affects the decimal places past the third decimal, which are not shown in our tables, so this interpretation can be made to our reported slopes without applying the formula.

With clustered data, ordinary correlation coefficients are not appropriate (Bland and Altman, 1994). For the clustered data, the correlation has both a within subjects component (Bland and Altman, 1995a) (do osteons with increasing B.Ar have increasing HC.Pm in the same bone specimen?) and a between subjects component (Bland and Altman, 1995b) (do bone specimens with increasing B.Ar have increasing HC.Pm?). We fitted the between subjects clustered Pearson correlation coefficient (Bland and Altman 1995b), which is closer to how researchers normally think about correlation.

Data from mature and subadult bones in the deer rib and humerus groups were each combined for the regression and correlation analyses because of sample sizes of only one or two sub-adult animals in each of these groups. Data from the black bear metatarsals and metacarpals were analyzed in terms of three groups: 1) immature bones, 2) mature bones, and 3) immature and mature bones combined. Consideration of the results of this analysis also focused on the combined data because the small samples ($n = 3$) in the immature groups were likely spuriously inflated correlation coefficients due to overfitting. Overfitting occurs when too few observations are available for the two variables used in the analysis, where the correlation becomes artificially high as the fit begins to approach a straight line through two points (perfect fit, or $r = 1.0$) regardless of the true association in the sample population.

A mixed effects linear regression model was also used to detect significant differences in HC.Pm/B.Ar between bones, and between smaller and larger osteons within each bone sample (the small/large cutoff was the mean osteon diameter for each sample). In these models, the data were limited to two groups, so the models were analogous to independent sample and paired t-tests, while accounting for the lack of independence due to nesting of the data. Since a large number of comparisons were made, the significance level was set at $P < 0.001$, providing some protection against an inflated alpha from multiple comparisons. The number of comparisons was too many to practically apply a formal multiple comparison adjustment. All P values are for a two-sided comparison. These additional statistical analyses were conducted with the Stata software. All other statistical analyses not using Stata or PAST software were conducted with StatView software (version 5, SAS Institute Inc., Cary, NC).

RESULTS

Osteon diameters (On.Dm) varied greatly in all bones, and this was the dominant factor governing On.Ar (total osteon area) and B.Ar (osteon wall area) because the range of Haversian canal diameters (HC.Dm) was much less (Fig. 2). This observation refers to absolute measures of size. Remodeling rates of Haversian canals and osteons are likely more similar with respect to surface area if the osteons are relatively symmetric. Consequently, in terms of remodeling rates per surface area, it is probable that the parameters shown in Figure 2 are more similar. Unfortunately, this possibility could not be fully evaluated in the present study.

For all samples with more than three bones, the nested least-squares correlation coefficients (r) are 0.95 or greater for the comparison between On.Ar and B.Ar, and for the comparison between On.Dm and B.Ar. These results are consistent with the strong relationships that would be expected when osteons are highly circular.

Regressions and potential allometric relationships

Results of regression analyses of HC.Pm versus B.Ar (indicated here as "HC.Pm/B.Ar") relationships for the

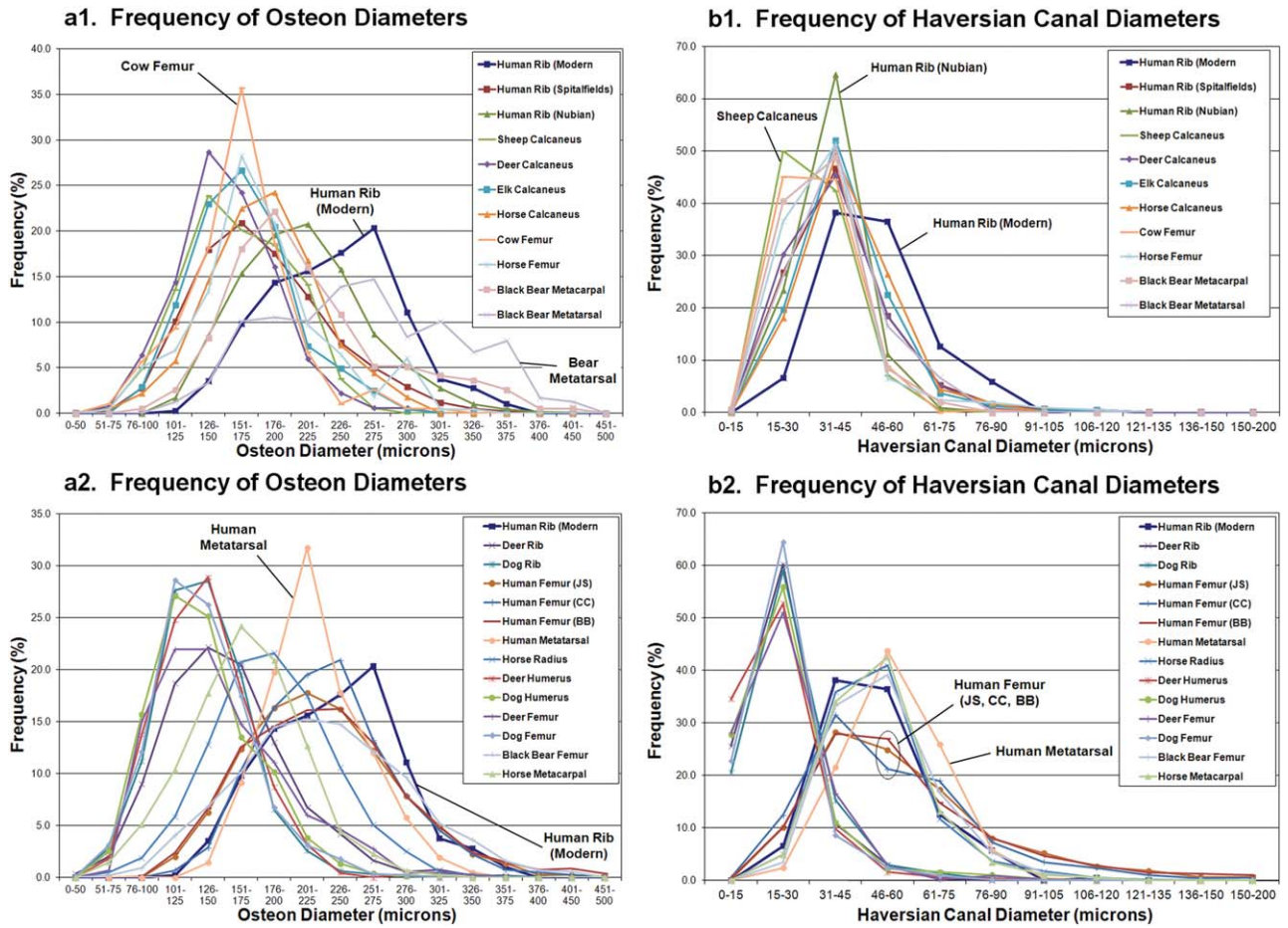

Fig. 2. (**a1–2**) Line plots of the range of osteon diameters (i.e., cement line diameters) in all bones. (**b1–2**) Line plots of the range of Haversian canal diameters in all bones. The bone samples were separated in a quasi-arbitrary fashion into two groups for the purpose of facilitating the viewing of the different curves. Modern human ribs are shown in both groups for comparison. Samples with mature and immature bones are shown with one curve that displays these combined data.

osteons in each bone type are shown in Table 2. Because the RMA analysis is currently not an appropriate test for the nested data, RMA slopes are only shown and discussed as they relate to the un-nested data.

Although four of the five rib groups showed positive allometry in terms of the RMA slopes, nearly 50% of the adult limb bone groups also showed positive allometry when negative allometry was expected (Table 2). Hence, regardless of the statistical method (LS showed negative allometry for nearly all specimens for the nested and un-nested analyses), it is not possible to distinguish ribs from limb bones based on the hypothesized allometric scaling relationships (Fig. 1). For example, the predicted positive allometry was shown in the RMA slopes of the modern and Spitalfields human ribs, but negative allometry was shown in the Nubian ribs. Furthermore, the RMA slopes of the human femora and metatarsal samples showed positive allometry and not the predicted negative allometry for these limb bones. The least-squares slopes obtained in the nested analysis (Table 2, left side) and un-nested analysis (Table 2, right side) also did not distinguish osteons from these samples of human ribs and limb bones.

The correlation coefficients reported in Table 2 in terms of the nested analysis show that over one-half of the samples with ≥ 5 specimens have moderate to high positive ($r \geq 0.45$) relationships between HC.Pm and B.Ar. Regression data in the sheep calcanei are a notable exception in this context—none of the regression analyses in this bone were statistically significant.

Figure 3 shows regression plots of HC.Pm/B.Ar (using un-nested data) for selected samples of human ribs and human femora. When considering the least-squares slopes, these plots demonstrate various degrees of negative scaling relationships (slopes <0.5), which are shown as solid lines.

Examination of data displayed in Figures 2 and 4 shows that the rib osteons do not extend to the extremes of the ranges of BS/BV dimensions shown by all the data of the other bone samples. However, the modern rib osteons tend to be generally larger and tend to span a broader size range than the most of the samples of limb bone osteons (Fig. 2a). By contrast, the size ranges of Haversian canals of rib osteons are not generally broader than the other non-rib samples, and the rib Haversian canals are not generally larger than the Haversian canals of limb bone osteons (Fig. 2b). This relative constraint in HC.Dm helps explain why the HC.Pm/B.Ar relationships are negatively allometric in nearly all bones when considered in terms of the least-squares regression coefficients.

TABLE 2. HC.Pm/B.Ar (BS/BV) relationships using log_{10}-transformed data from each group, which are displayed as least-squares (LS) and reduced major axis (RMA) regressions

	Mixed effects (nested) analysis results					Un-nested analysis results							
	No. Osteons[a]	LS slope	*r*	*P*	95% CI	LS slope	*r*	*P*	95% CI	RMA slope	*r*	*P*	95% CI
Human Ribs													
Modern	398 (9)	0.45	0.33	s	0.39–0.51	0.45	0.61	s	0.39–0.50	0.73	0.61	s	0.67–0.79
Spitalfields	5,244 (223)	0.34	0.61	s	0.32–0.35	0.33[b]	0.56	s	0.32–0.34	0.59	0.56	s	0.57–0.60
Nubian	1,792 (80)	0.21	0.75	s	0.19–0.23	0.22	0.49	s	0.20–0.24	0.45	0.49	s	0.44–0.47
Nonhuman ribs													
Deer (All)	546 (6)	0.30	0.72	s	0.26–0.35	0.35[b]	0.54	s	0.30–0.39	0.64	0.54	s	0.59–0.69
Dog	963 (6)	0.26	0.73	s	0.21–0.31	0.28[b]	0.34	s	0.23–0.34	0.85	0.34	s	0.79–0.90
Human limb bones													
Femur (JS)	1,784 (12)	0.38	0.63	s	0.34–0.42	0.40[b]	0.45	s	0.36–0.43	0.87	0.45	s	0.84–0.90
Femur (CC)	9,941 (213)	0.42	0.62	s	0.40–0.44	0.44[b]	0.45	s	0.43–0.46	0.99	0.45	s	0.97–1.01
Femur (BB)	1,560 (26)	0.38	0.27	s	0.34–0.41	0.34[b]	0.42	s	0.31–0.38	0.83	0.42	s	0.79–0.86
Metatarsal	208 (15)	0.36	0.17	s	0.26–0.45	0.35[b]	0.44	s	0.25–0.44	0.79	0.44	s	0.69–0.86
Nonhuman limb bones													
Calcaneus													
Sheep	184 (7)	0.01	0.24	0.70	−0.05 to 0.08	0.01	0.03	0.70	−0.05 to 0.08	0.43	0.03	0.70	0.37−1.34
Deer	672 (10)	0.13	0.38	0	0.09−0.17	0.12[b]	0.22	s	0.08−0.16	0.56	0.22	s	0.51−0.60
Elk	244 (7)	0.14	0.31	s	0.07−0.21	0.15[b]	0.24	s	0.07−0.22	0.61	0.24	s	0.52−0.68
Horse	227 (7)	0.21	0.83	s	0.15−0.28	0.21	0.39	s	0.15−0.28	0.55	0.39	s	0.46−0.62
Radius													
Horse	2,344 (10)	0.22	0.08	s	0.20−0.24	0.21	0.40	s	0.19−0.23	0.52	0.40	s	0.50−0.54
Humerus													
Deer (all)	436 (5)	0.24	0.70	s	0.16−0.31	0.17[b]	0.21	s	0.09−0.24	0.80	0.21		0.71−0.87
Dog	756(6)	0.37	0.75	s	0.31−0.43	0.37[b]	0.45	s	0.32−0.42	0.83	0.45		0.77−0.89
Femur													
Deer	433 (4)	0.42	0.96	s	0.36−0.48	0.49	0.65	s	0.43−0.54	0.75	0.65	s	0.69−0.80
Cow	193 (20)	0.14	0.34	s	0.07−0.21	0.14	0.27	s	0.07−0.21	0.52	0.27	s	0.42−0.60
Horse	216 (20)	0.32	0.61	s	0.27−0.38	0.34	0.60	s	0.28−0.40	0.56	0.60	s	0.49−0.63
Dog	891 (6)	0.29	0.78	s	0.25−0.33	0.35[b]	0.48	s	0.30−0.39	0.72	0.48	s	0.67−0.78
Black Bear (Im)	1,215 (31)	0.07	0.50	s	0.04−0.09	0.07	0.17	s	0.05−0.10	0.42	0.17	s	0.39−0.45
Black Bear (M)	780 (16)	0.09	0.19	s	0.06−0.12	0.09	0.20	s	0.06−0.12	0.45	0.20	s	0.42−0.48
Metacarpal													
Black Bear (Im)	83 (3)	0.17	0.83	s	0.04−0.29	0.17	0.30	s	0.05−0.29	0.57	0.30	s	0.42−0.70
Black Bear (M)	111 (4)	0.20	0.95	s	0.08−0.31	0.31	0.55	s	0.22−0.40	0.56	0.55	s	0.48−0.65
Black Bear (All)	194 (7)	0.13	0.64	s	0.05−0.22	0.20	0.38	s	0.13−0.27	0.53	0.38	s	0.45−0.60
Horse	2,458 (9)	0.10	0.96	s	0.08−0.11	0.10	0.22	s	0.08−0.11	0.44	0.22	s	0.42−0.46
Metatarsal													
Black Bear (Im)	68 (3)	0.13	0.26	0.04	0.01−0.25	0.13	0.25	0.04	0.00−0.25	0.52	0.25	0.05	0.35−0.67
Black Bear (M)	170 (6)	0.19	0.87	s	0.11−0.27	0.24	0.47	s	0.17−0.31	0.52	0.47	s	0.44−0.59
Black Bear (All)	238 (9)	0.19	0.87	s	0.12−0.26	0.23	0.45	s	0.17−0.29	0.52	0.45	s	0.45−0.58

At left are results of the mixed effects (nested) analysis and at right are the results obtained when using all data from all specimens as if they were independent (i.e., un-nested analysis).

[a] The number in parentheses indicates the number of subjects (see Table 1).

[b] Indicates bones in the un-nested analysis where the LS slope shows negative allometry but the RMA slope shows positive allometry.

Isometry = least-square (LS) or RMA slope of 0.5. By definition, negative allometry and positive allometry do not contain the slope of 0.5 within the 95% confidence intervals. s = significant *P* values at <0.01. All but two nested and four un-nested *r* values are significant at $P < 0.01$. CI = 95% confidence intervals; RMA = reduced major axis regression; Im = immature; M = mature; All = immature and mature.

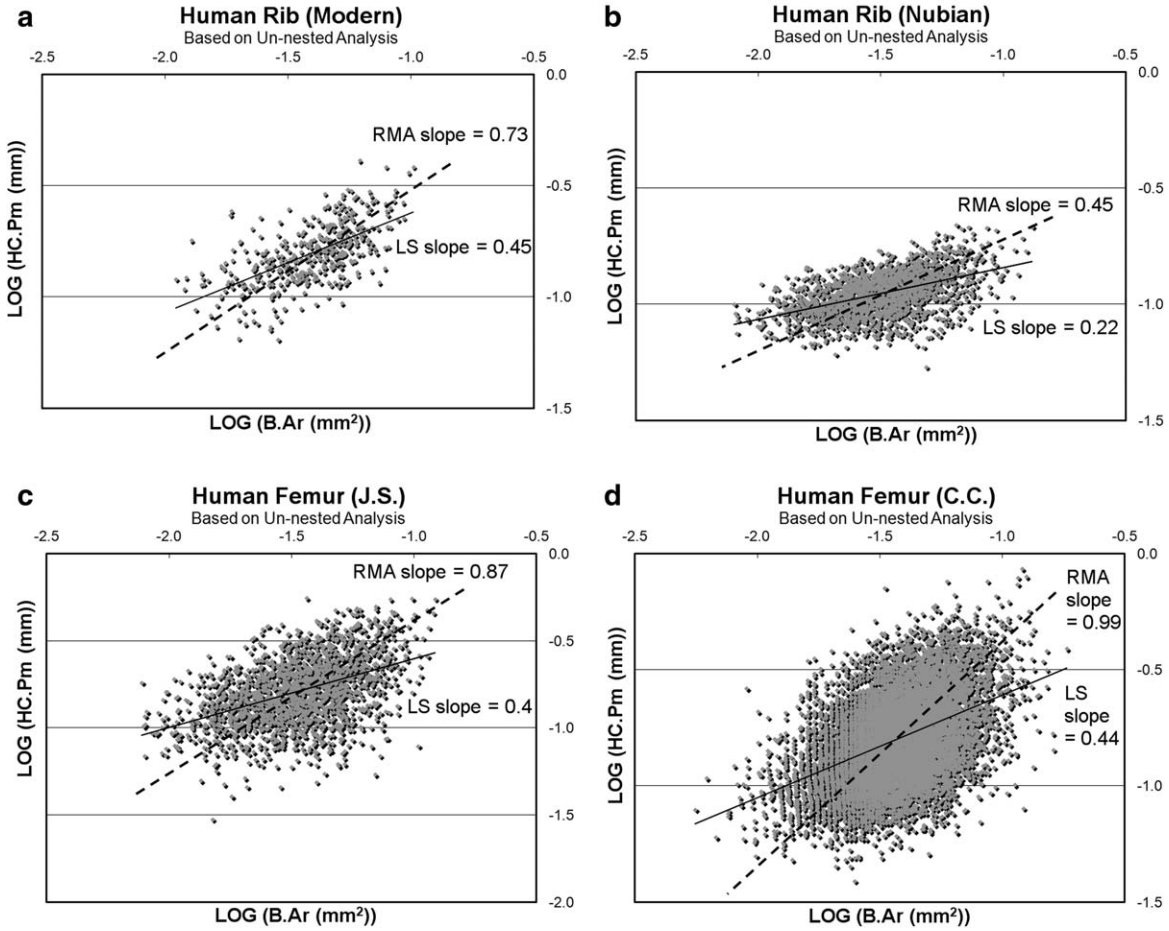

Fig. 3. Least-squares (LS, solid lines) and reduced major axis (RMA, dashed lines) trend lines of HC.Pm versus B.Ar (BS/BV) using $\log_{10}$-transformed data from: **a**. modern human ribs, **b**. human Nubian ribs, **c**. human femora (JS), and **d**. human femora (CC). These plots show all of the data from the individual osteons from each specimen (i.e., un-nested analysis). Note that in these four graphs the intervals that sub-divide the axes are asymmetric and the axes are also not equivalent between groups; some were adjusted to enhance the display of the data.

Correlations among additional osteonal dimensions

Table 3 shows various additional osteon dimensional relationships using least-squares analysis of non-transformed data that are nested within each bone. These results illustrate relationships of osteon size with respect to HC.Pm (BS), B.Ar (BV), and HC.Pm/B.Ar (BS/BV) data. These results demonstrate that these parameters are not consistently correlated and, notably, osteon size is not consistently correlated with the HC.Pm/B.Ar ratio.

Comparisons in cases of low versus high strain, and when there are different osteon morphotypes

It was also predicted that the rib osteons would have proportionally larger Haversian canals (i.e., greater HC.Ar/On.Ar = % canal area) than the osteons in the dorsal ("compression"; high strain) cortices of the sheep, deer, elk, and equine calcanei. By contrast, Haversian canals that are proportionally more similar in size were also anticipated in the osteons of the ribs and in these plantar ("tension"; low strain) calcaneal cortices. However, as shown by data summarized in Figure 5, none of these possibilities appear to be supported. In other words, proportionally larger HC size is not a distinguishing characteristic of rib osteons. In fact, and also contrary to our predictions, Figure 5b shows that compared with ribs there is a relatively greater percentage of osteons (we predicted smaller percentages) with proportionally larger canals in the highly strained dorsal cortices of the calcanei ($P < 0.05$ in all comparisons with modern human ribs). Similar results are found when rib osteons are compared with the samples of human femora (data not shown).

Differences in allometric scaling of HC.Pm with B.Ar were also not evident when osteons from habitual "tension" and "compression" cortices were compared in the sheep, deer, elk and equine calcanei and equine radii (data not shown). These results diminish the possibility that dimensional allometry is influenced by the presence of differences in osteon morphotypes that occur between these regions.

HC.Pm/B.Ar data and paired comparisons between and within samples

Table 4 shows means and standard deviations of the HC.Pm/B.Ar ratio for all bone samples. Results of these paired comparisons (data nested for each bone)

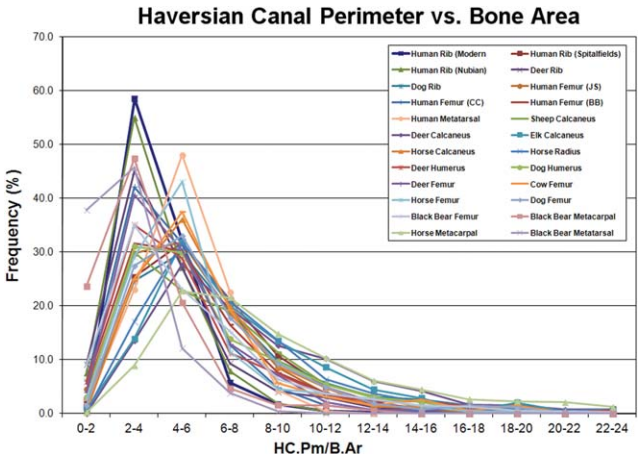

Fig. 4. Line plots of the range of HC.Pm/B.Ar (BS/BV) data in all bones. The fact that the rib osteons do not have relatively larger values when compared with the limb-bone osteons was not expected in the context of the hypotheses (Fig. 1). Each sample with mature and immature bones is shown with one curve that displays these combined data.

demonstrate that in most cases these mean data differ between the groups. A separate nested analysis of small versus large osteons (cutoff = mean diameter) in each sample shows that HC.Pm/B.Ar was significantly greater ($P < 0.01$) in small osteons than in large osteons for all comparisons. This result again is consistent with the negative allometries of nearly all of the least-squares regressions.

Potential growth and age influences

In non-human bones, the sample of black bear femora is the most robust in terms of sample size and greatest accuracy of animal ages. HC.Pm/B.Ar regressions from the nested data from skeletally immature black bear femora (i.e., 5 years and younger) showed a moderate correlation ($r = 0.5$) that was negatively allometric (LS slope = 0.07). This correlation was weaker in the mature black bear femora ($r = 0.19$), where it was also negatively allometric (LS slope = 0.09) (Table 2). This suggests no important age or growth effects in BS/BV in this non-human limb bone. Finally, the analyses conducted in some of the human samples also did not reveal any clear or consistent effect of aging (Table 5).

DISCUSSION

We expected differences in osteon BS/BV scaling relationships (expressed here as HC.Pm vs. B.Ar) between osteons of ribs and limb bones because of the different mechanical, physiological, and metabolic functions of these bones. Contrary to our prediction, however, the samples of rib osteons could not be distinguished from the samples of limb bone osteons based on the predicted allometric scaling relationships. This is clear when considering that even though 80% (four of five) of the rib groups showed positive allometry in terms of the RMA slopes, only ~50% of the adult limb bone groups showed the expected negative allometry. In the rib groups, the Nubians are the exception because they showed negative allometry of their HC.Pm/B.Ar relationships in terms of the RMA analysis. It is unclear if the relatively poor health of the Nubian sample (Mulhern, 2000), or perhaps their relatively increased physical activity, contributed in distinguishing this group from the other human rib samples. Nevertheless, limb and rib bones are indistinguishable based on the hypothesized osteon BS/BV scaling relationships. Growth, sex, and aging also did not appear to have a clear effect in changing HC.Pm/B.Ar relationships in the cases where these factors could be evaluated.

Limitations of this study include the different tissue processing and microscope imaging methods that were used (e.g., light microscopy vs. backscattered electron imaging; Table 1). The tissue preservation prior to imaging (e.g., dry vs. moist/fresh) was also not consistent. Furthermore, we made no attempt to systematically and independently re-evaluate any of the images in order to assess error among the various samples and investigators. Load histories of the bones also differ and in most cases are not well characterized (the calcanei and equine radii are exceptions). Although we used approved ASBMR nomenclature and methods when estimating BS/BV from 2D osteon data (HC.Pm/B.Ar), these 2D parameters are only surrogates for BS/BV data from entire secondary osteons. A logical future study would be to examine the hypothesis of different scaling relationships in a three-dimensional analysis of entire osteons from ribs and limb bones using high resolution microcomputed tomography (Carter et al., 2013) within the same subjects of known age. However, these limitations of the present study are typical in investigations that consider and assemble histomorphological data from various studies for comparative analyses of anthropoid and non-anthropoid bones (Mulhern and Ubelaker, 2012). Therefore, we consider our data to be useful because in the various anthropoid and non-anthropoid bones the results are generally consistent—dimensional allometry of HC.Pm/B.Ar does not distinguish osteons from rib and limb bones. The overall conclusions that are drawn from these data therefore do not seem to be confounded by these limitations or by species differences in any obvious way.

Another limitation is that we did not examine ribs and limb bones from the same individuals. Stronger evidence for allometry of osteon size and canal size might be observed in ribs and long bones when bones from the same individual are compared. This is because inter-skeletal variability might be overwhelming intra-skeletal differences (Jepsen et al., 2011). Additional studies are needed in this context.

In terms of un-nested data, nearly all adult bones (10 of 12 groups) with moderate or stronger correlations ($r \geq 0.45$) showed negative allometries based on their least-squares slopes (Table 2, right side). This finding can be explained by data showing that intra- and inter-species variability in the size of Haversian canals is generally constrained (Fig. 2b) even though there is comparatively substantial intra- and inter-species variability in osteon size (Fig. 2a). Consequently, even when overall osteon size (diameter) variations are likely mechanically advantageous, the apparent importance of keeping porosity low may be why negative allometry or weak positive allometry is shown by the least-squares slopes in most bones with correlations that are $\geq$0.45. This mechanical priority is supported by data showing that small changes in porosity lead to disproportionately large reductions in bone strength and stiffness. Hence,

TABLE 3. Additional osteon dimensional relationships using nontransformed data

	On.Dm vs. HC.Dm	On.Dm vs. HC.Pm/B.Ar	HC.Dm vs. B.Ar
Human Ribs			
Modern	NS	−0.86(0.13)	NS
Spitalfields	0.61	−0.81	0.55
Nubian	0.78	−0.70	0.77
Nonhuman ribs			
Deer	NS	NS	0.76 (0.08)
Dog	0.78 (0.07)	NS	0.76 (0.08)
Human limb bones			
Femur (JS)	0.70	−0.57(0.15)	0.62
Femur (CC)	0.68	−0.49	0.67
Femur (BB)	NS	−0.73	NS
Metatarsal	NS	−0.62(0.09)	NS
Nonhuman limb bones			
Calcaneus			
Sheep	NS	NS	NS
Deer	NS	NS	NS
Elk	NS	NS	NS
Horse	0.87	NS	0.85
Radius			
Horse	NS	−0.68(0.15)	NS
Humerus			
Deer	NS	NS	NS
Dog	NS	NS	NS
Femur			
Deer	0.96	NS	0.93
Cow	NS	−0.83	NS
Horse	0.71	NS	0.75
Dog	0.90	NS	0.90
Black Bear (immature)	0.47	−0.85	0.44
Black Bear (mature)	NS	−0.69	NS
Metacarpal			
Black Bear (immature)	NS	NS	NS
Black Bear (mature)	0.95	NS	0.93(0.07)
Black Bear (all)	NS	NS	NS
Horse	−0.98(0.08)	−0.92(0.09)	−0.98(0.08)
Metatarsal			
Black Bear (immature)	NS	NS	NS
Black Bear (mature)	0.87	NS	0.89
Black Bear (all)	0.89	−0.75(0.15)	0.88

Correlation coefficients shown with P values in parentheses are trends or tendencies ($0.05 < P \leq 0.15$); otherwise the P values of the significant correlations are all $P \leq 0.05$.
NS = nonsignificant.

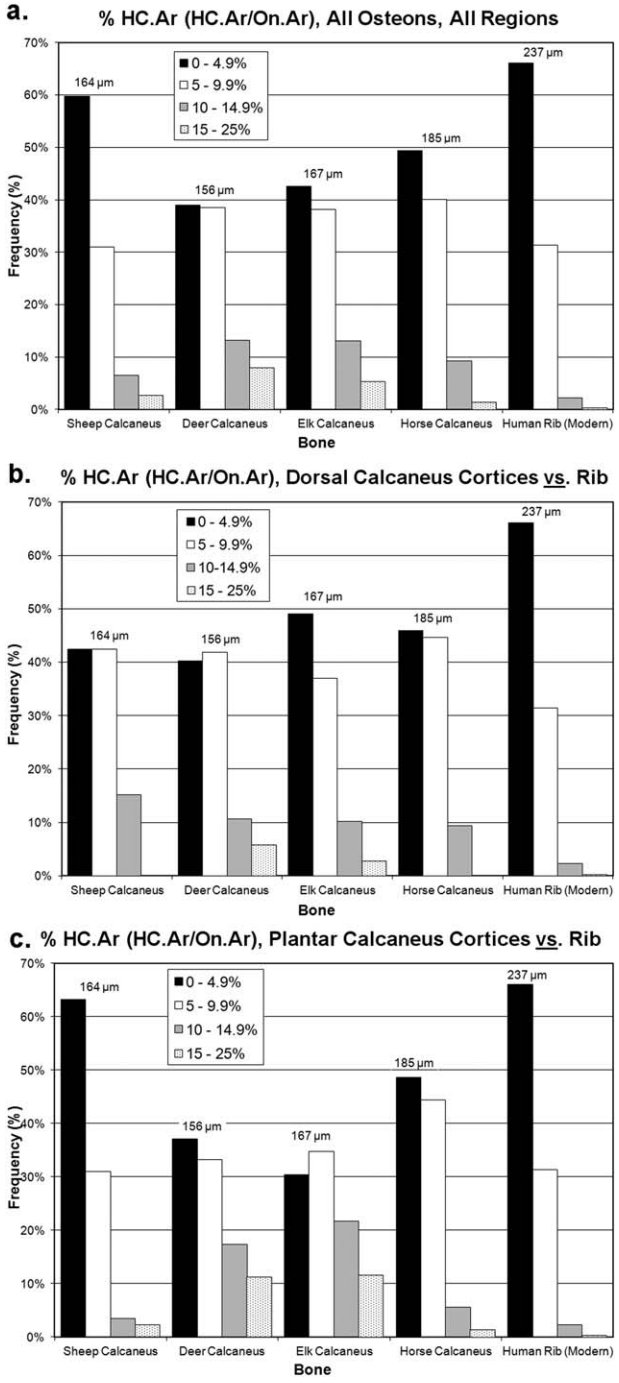

Fig. 5. (**a**) Frequencies of %HC.Ar (HC.Ar/On.Ar) for each of the calcanei and modern human ribs. These data also represent the percent of osteon in-filling (re-filling). (**b**) The frequencies of %HC.Ar (HC.Ar/On.Ar) for the dorsal ("compression") cortex of all calcanei compared with the frequency of %HC.Ar (HC.Ar/On.Ar) of the modern human ribs. Compared with the plantar regions, remodeling in the dorsal region occurs at a lower rate in adults (Skedros et al. 1997, 2001, 2004). (**c**) The frequencies of %HC.Ar (HC.Ar/On.Ar) for the plantar ("tension") cortex of all calcanei compared with the frequency of %HC.Ar (HC.Ar/On.Ar) of the modern human ribs. In the plantar cortex of mature bones, and presumably also in the rib, the rate of active remodeling is higher than in the dorsal ("compression") cortex of the calcanei (Skedros et al. 1997, 2001, 2004). For A–C: The number above each bone data set indicates the mean osteon diameter (On.Dm) in microns (µm).

porosity generally has a deleterious effect on mechanical properties of bone (Currey, 1988; Martin and Boardman, 1993; Turner, 2002; Currey et al., 2004). However, this interpretation seems less palatable when considering the fact that six of these 10 groups had RMA slopes that were positively allometric (Table 2, right side). This demonstrates that biomechanical interpretations can be dramatically different when considering the least-squares versus RMA slopes. For example, the RMA slopes do not consistently show negative allometry in the non-human rib osteons even though their rib loading is likely more substantial than in humans (Simons, 1999).

Several investigators have favored the hypothesis that bone lining cells (BLCs), not osteocytes, manipulate

TABLE 4. Comparisons of HC.Pm/B.Ar data between groups

	Mean	Std. dev.	Statistically significant ($P \leq 0.001$) from:
Human ribs			
Modern	4.01	1.55	2–6, 8, 10–13, 15–20, 23–25
Spitalfields	5.91	3.05	1, 3–10, 14–24
Nubian	3.84	1.63	1–2, 4–18, 20–24
Nonhuman ribs			
Deer	3.94	2.28	1–3, 5–14, 18–19, 21–25
Dog	6.60	4.14	1–4, 6–15, 18–19, 21–25
Human limb bones			
Femur (JS)	5.43	2.72	1–5, 10–25
Femur (CC)	4.53	2.24	2–5, 10–21, 23–25
Femur (BB)	5.49	3.32	1–5, 10–25
Metatarsal	5.13	1.60	2–5, 10–21, 23–25
Nonhuman limb bones			
Calcaneus			
Sheep	6.51	4.24	1–9, 11–17, 20–22, 24–25
Deer	8.49	5.77	1, 3–10, 14–18, 20–24
Elk	7.35	3.86	1, 3–10, 14–25
Horse	6.03	3.25	1, 3–10, 14–25
Radius			
Horse	7.35	4.68	2–13, 15–20, 22–23, 25
Humerus			
Deer (all)	4.10	2.61	1–3, 5–14, 17–25
Dog	5.94	3.58	1–3, 6–14, 18–19, 21–25
Femur			
Deer	3.22	0.97	1–3, 6–15, 18–19, 21–25
Cow	6.22	4.73	1–9, 11–17, 19–22, 24–25
Horse	5.34	2.88	1–2, 4–9, 12–18, 20–22, 24
Dog	6.00	3.42	1–3, 6–15, 18–19, 21–25
Black Bear (immature)	5.48	4.47	2–13, 15–20, 22–23, 25
Black Bear (mature)	6.38	5.82	2–6, 8, 10–21, 23–25
Metacarpal			
Black Bear (all)	3.46	1.74	1–9, 11–17, 20–22, 24–25
Horse	10.62	9.71	1–13, 15–20, 22–23, 25
Metatarsal			
Black Bear (all)	3.35	2.83	1, 4–10, 13–18, 20–24

The numbers at the far right refer to the bones in the list in ascending order from top to bottom (where #1 is modern human rib and #25 is black bear metatarsal).

TABLE 5. Age analyses of HC.Pm/B.Ar (BS/BV) relationships using logged data from human rib (Spitalfields) and human femora (JS; CC)

	No. osteons	LS slope[a]	*r*	*P*	95% CI	RMA slope[a]
Human rib (Spitalfields)						
<50 years ($n = 68$)	1,479	0.33[b]	0.55	<0.01	0.31–0.36	0.61[b]
≥50 years ($n = 152$)	3,615	0.34	0.70	<0.01	0.33–0.36	0.49
<70 years ($n = 158$)	3,624	0.34[b]	0.57	<0.01	0.32–0.36	0.60[b]
≥70 years ($n = 62$)	1,470	0.33	0.70	<0.01	0.30–0.36	0.47
Human femur (JS)[c]						
<60 years ($n = 5$)	762	0.39[b]	0.67	<0.01	0.33–0.45	0.58[b]
≥60 years ($n = 7$)	1,022	0.37[b]	0.57	<0.01	0.33–0.42	0.65[b]
Human femur (CC)						
<50 years ($n = 25$)	1,185	0.45	0.44	<0.01	0.40–0.50	1.02
≥50 years ($n = 188$)	8,756	0.42[b]	0.66	<0.01	0.40–0.44	0.66[b]
<70 years ($n = 117$)	5,604	0.40[b]	0.53	<0.01	0.38–0.43	0.66[b]
≥70 years ($n = 96$)	4,337	0.44[b]	0.67	<0.01	0.41–0.47	0.66[b]

[a] Allometric relationships are shown by these slopes: 1) isometry is equal to 0.5, 2) negative allometry is <0.5, and 3) positive allometry is >0.5. Positive and negative allometry do not contain 0.5 in the 95% CIs.
[b] Cases where the LS slope shows negative allometry but the RMA slope shows positive allometry.
CI = 95% confidence intervals; n = the number of individuals in each subset. For other abbreviations see legend of Table 2.
[c] The Human Femur (JS) is analyzed as <60 and >60 years because: 1) when using the 50 year cut-off the <50-year-old group had only three individuals, and 2) when using the 70-year cut-off only one individual was >70 (71 years old).

calcium solubility on quiescent surfaces in response to calcium-regulating hormones (Staub et al., 1989; Parfitt, 1987, 1993; Talmage et al., 2000; Qiu et al., 2002). A plausible mechanism whereby modification of the osteonal in-filling process is coupled to BLC-mediated calcium exchange involves variations in osteocyte production of sclerostin—a glycoprotein that appears to be the strongest regulator of the extent of osteonal in-filling

(Skedros et al., 2011a; Power et al., 2012). In this perspective we initially suspected that, compared with limb bone osteons, rib osteons would have enhanced efficiency of non-remodeling calcium exchange mechanisms (e.g., isoionic and heterionic exchange; see Appendix) (Heaney, 2003) that would be detected in 2D by their comparatively proportionally larger Haversian canal areas with increased osteon size. But the failure of our data to distinguish rib versus limb bone osteons in this context is consistent with the conclusion that, when needed, the mobilization of calcium across the quiescent osteonal surfaces is sufficient for short-term needs (e.g., on the scale of hours, such as between meals) without differentially modifying osteonal porosity between ribs and limb bones. Conventional wisdom is that greater calcium demands are primarily satisfied by resorption of trabecular (cancellous) bone surfaces, which is accomplished by hemi-osteonal remodeling (Parfitt, 2010; Qiu et al., 2010). However, a recent study suggests that the maintenance of bone balance is more efficient for intra-cortical remodeling in the rib than for endo-cortical or cancellous remodeling at any other site (Qiu et al., 2010). Nevertheless, in situations when cortical bone of ribs and limb bones might be an important calcium source, the activation of osteonal remodeling appears to be an important means for mobilizing relatively large amounts of calcium for greater demands or long-term needs (e.g., lactation, pregnancy, and dietary deficiency) (Hillman et al., 1973; Vajda et al., 1999; Bowman and Miller, 2001; Heaney, 2003; Parfitt, 2010). But there is evidence that during the reproductive cycle significant amounts of calcium can be reversibly removed from the bone matrix via osteocytic osteolysis (i.e., independent of osteoclastic resorption) of the perilacunar and pericanalicular spaces (Qing et al., 2012). However, this has been definitively shown to occur in mice where, to our knowledge, osteonal remodeling does not occur in natural conditions. Consequently it remains unclear what the relative importance of osteon-mediated remodeling versus osteocytic osteolysis might be in species that have the capacity for extensive osteonal remodeling.

Our assumption that optimization for calcium exchange in ribs would be seen as positive allometry in their osteonal BS/BV relationships is also likely fundamentally flawed in the context of potential variations in osteonal histomorphological characteristics. For example, we based our main predictions on the idea that fluid flux across the osteonal wall can be viewed as a convective-based process that is relatively simple and similar for all osteons that we studied. There are aspects of osteon microporosity and other matrix characteristics that could exhibit phenotypic plasticity and, in turn, could influence trans-osteonal fluid-flow dynamics and calcium exchange across the osteon canal surface (see Appendix). These include variations in the number of dendrites per osteocyte (which is reflected in canalicular density), the trans-osteonal arrangement of osteocytes and their dendrites, and intercellular gap junction connectivity (Ferretti et al., 1999; Okada et al., 2002; Mishra and Knothe Tate, 2003; Ascenzi et al., 2004; Palumbo et al., 2004; Kerschnitzki et al., 2011). The blood-bone barrier formed by BLCs is also not simple (Wang et al., 2000). It is possible that these morphologic characteristics are non-equivalent in osteons from different cortical regions, bones, and/or species. The existence of this osteonal non-equivalence would invalidate the use of BS/BV data as the sole criterion for determining if there might be differences in calcium exchange in rib versus limb-bone osteons.

We postulate that non-equivalent osteon matrix microporosities, which might be associated with different osteon morphotypes (Skedros et al., 2009, 2011b), could be present in some of the osteons that were evaluated in the present study. This could include species or load-related differences in lacuna-canalicular geometries. We could not distinguish these putative differences because none of the osteons were analyzed at the high magnifications and imaging conditions (e.g., confocal microscopy) that are required for this analysis. Nevertheless, these possibilities raise a cautionary flag—non-uniformities in characteristics of matrix microporosities between osteons in different bones or between different regions of the same bone could confound attempts to identify relationships between HC.Pm and B.Ar and the trans-canal and trans-osteonal fluid flow dynamics that effect molecular and nutrient transport and exchange.

Although the data shown in Table 2 generally show statistically significant correlations of HC.Pm with B.Ar across broad ranges of osteon size, the sheep calcanei are a glaring exception because of their lack of a HC.Pm/B.Ar relationship. Additionally, the correlations of HC.Pm and B.Ar in many of the other limb bones are weak. These data suggest that a functional relationship between HC.Pm and B.Ar is not consistent and, if present, is typically not strong. With respect to data in sheep calcanei, it is possible that the less rigorous ambulatory activities of the domesticated sheep used in this study does not evoke a frequency of osteonal remodeling that is sufficient for detecting relationships between the degree of osteon in-filling and osteon size. This contrasts with the higher rate of osteonal renewal that has been previously reported in the calcanei of the wild animals (elk and deer) and domesticated horses that were also examined in the present investigation (Skedros et al., 2011c). This explanation is discussed further in prior studies (Skedros et al., 2011a,c).

Finally, in Figure 2a,b there appears to be bimodal distributions of Haversian canal size that reflect animal size. It is possible, given the fact that the larger species in our samples also tend to live longer, that an association or even minor relation between either body size or animal longevity could be made with osteon size and could potentially affect osteon surface-volume scaling relationships. However, we could not fully evaluate this possibility because the mass and age data were not available for all animals.

In summary, the results of this study do not provide evidence that BS/BV scaling, expressed as HC.Pm/B.Ar in a 2D analysis, reflects a rib versus limb bone dichotomy whereby calcium exchange might be preferentially enhanced across quiescent canal surfaces of rib osteons. Non-remodeling calcium-exchange mechanisms (e.g., isoionic and heterionic; and possibly osteocytic osteolysis) must therefore be sufficient in terms of the role that ribs and limb bones might have in satisfying calcium demands of typical daily living. Consequently, while our data show that the use of dimensional allometry in HC.Pm/B.Ar relationships does not support a dichotomy in the capacity for calcium exchange across quiescent canals of mature osteons in ribs versus limb bones, this possibility cannot be summarily ruled out if osteons are not equivalent in other matrix characteristics that could influence non-remodeling calcium exchange. Additional studies using data from entire secondary osteons are now needed to more rigorously test these hypotheses.

ACKNOWLEDGMENTS

The authors thank Roy Bloebaum, Kendra Keenan, Zoe Morris, Mark Nielsen, Dennis Bramble, Susan Pfeiffer, Sara Gookin, David Weyland, Andreas Bernhard, Michael Hahn, Walter Klippel, Lee Meadows Jantz, Murray Marks, and David Burr for laboratory facilities, other technical support for obtaining the data, and/or criticisms of the manuscript. Greg Stoddard was consulted for assistance with statistical analyses. The opinions stated in this paper are the views of the authors and should not be construed as official or as reflecting the views of the Department of Defense, its branches, or the Armed Forces Medical Examiner System.

APPENDIX: NUTRIENT/MOLECULAR EXCHANGE/ DELIVERY ACROSS THE HAVERSIAN CANAL SURFACE AND WITHIN THE OSTEON WALL

Trans-osteonal calcium exchange and nutrient delivery could be affected by: 1) Haversian canal size, 2) osteon size, 3) capillary number, 4) capillary diameter, 5) size of red blood cell (nucleated vs. non-nucleated in some species), 6) osteon "morphotype" (i.e., distinctive collagen/lamellar patterns) (Skedros et al., 2009), 7) lacuna-canalicular morphologies, 8) osteocyte density, 9) viability of osteocytes and bone lining cells (BLCs), and other aging effects, 10) habitual loading of the specific bone or bone region (e.g., low strain with increased cycles vs. high strain with decreased cycles; or tension vs. compression), and 11) the possibility that the cement line might not be a complete barrier to nutrient delivery via interstitial fluid flow (Haines et al., 1983; Curtis et al., 1985).

Metz et al. (2003) considered two mechanisms to explain the regulation of osteonal in-filling, and both involved a possible role for the density of osteocytes in forming the osteon wall. Similar to a basic assumption of the present study, these mechanisms assume unidirectional nutrient transfer from the Haversian canal into the osteon wall. Because the cement line is generally considered an effective barrier to significant nutrient transport, all osteocytes within an osteon must receive nutrients from the Haversian canal (Qin et al., 1999; Wang et al., 2000). The first mechanism involves transport across the Haversian canal surface. The second mechanism involves transport within the osteon wall. Both mechanisms can be modified in ways that are independent of in-filling and can influence BS/BV relationships; but these potential modifications (e.g., adjustments in lacuna-canalicular conduit geometries and densities) were not analyzed in the present study.

As summarized by Metz et al. (2003), nutrient flow through the blood vessel in the Haversian canal and transport out of the vessel and across the Haversian canal surface (i.e., the nutrient transport surface) must be adequate to support the viability of all osteocytes in the osteon wall. This is important because if osteocyte signals (e.g., the osteocyte-mediated production of sclerostin (Power et al., 2012)) could be modified to provide a larger Haversian canal, then this could allow for a larger blood vessel (or more than one blood vessel). This results in greater blood flow and greater surface area for nutrient transport into the osteon wall. If the radius of the Haversian canal doubles, then the nutrient transfer surface also doubles, but the flow rate through the larger blood vessel increases substantially more. In fact, for an idealized case, these investigators pointed out that flow rate through this hypothetically larger blood vessel could increase by a factor of 16 because, to the extent that Poiseuille's Law applies, fluid flow increases in proportion to $(\text{radius})^4$ of the tube (vessel). This is an important issue because it is another potential osteonal morphological characteristic that can confound simple interpretations of the physiology of BS/BV scaling relationships. In fact, there are data showing that progressive age-related remodeling of a bone's cortex can influence bone vascularity. In a study of the vascular network of an ontogenetic series of canine tibiae, Marotti and Zallone (1980) noted that as secondary osteons are formed and their canals narrow, there is a progressive reduction in the number of vessels in each canal. We know of no evidence that there are differences in the number of capillaries in Haversian canals of osteons from human ribs and limb bones examined in the present study. The only other reported observation that we are aware of that suggests that this might occur, but is unusual, is the mention by Chinsamy-Turan (2005). Furthermore we know of no data regarding the relationship between vessel diameter and Haversian canal diameter.

LITERATURE CITED

Amprino R, Marotti G. 1964. A topographic quantitative study of bone formation and reconstruction. In: Blackwood H, editor. Bone and tooth. London: Pergamon Press. p 21–33.

Andriacchi T, Schultz A, Belytschko T, Galante J. 1974. A model for studies of mechanical interactions between the human spine and rib cage. J Biomech 7:497–507.

Ascenzi MG, Andreuzzi M, Kabo JM. 2004. Mathematical modeling of human secondary osteons. Scanning 26:25–35.

Banks WJ, Glenwood PE, Kainer RA. 1968. Antler growth and osteoporosis: morphological and morphometric changes in the costal compacta during the antler growth cycle. Anat Rec 162:387–398.

Baxter BJ, Andrews RN, Barrell GK. 1999. Bone turnover associated with antler growth in red deer (*Cervus elaphus*). Anat Rec 256:14–19.

Bellemare F, Jeanneret A, Couture J. 2003. Sex differences in thoracic dimensions and configuration. Am J Respir Crit Care Med 168:305–312.

Bland JM, Altman DG. 1994. Correlation, regression, and repeated data. BMJ 308:896.

Bland JM, Altman DG. 1995a. Calculating correlation coefficients with repeated observations: Part 1—Correlation within subjects. BMJ 310:446.

Bland JM, Altman DG. 1995b. Calculating correlation coefficients with repeated observations: Part 2—Correlation between subjects. BMJ 310:633.

Bowman BM, Miller SC. 2001. Skeletal adaptations during mammalian reproduction. J Musculoskel Neuron Interact 1:347–355.

Busse B, Djonic D, Milovanovic P, Hahn M, Puschel K, Ritchie RO, Djuric M, Amling M. 2010a. Decrease in the osteocyte lacunar density accompanied by hypermineralized lacunar occlusion reveals failure and delay of remodeling in aged human bone. Aging Cell 9:1065–1075.

Busse B, Hahn M, Schinke T, Puschel K, Duda GN, Amling M. 2010b. Reorganization of the femoral cortex due to age-, sex-, and endoprosthetic-related effects emphasized by osteonal dimensions and remodeling. J Biomed Mater Res A 92:1440–1451.

Cagle DJ. 2011. Investigation of respiration induced strain caused on the rib. Mechanical Engineering Thesis. Ohio: The Ohio State University.

Carter Y, Thomas CD, Clement JG, Peele AG, Hannah K, Cooper DM. 2013. Variation in osteocyte lacunar morphology and density in the human femur: a synchrotron radiation micro-CT study. Bone 52:126–132.

Chinsamy-Turan A. 2005. The microstructure of dinosaur bone: deciphering biology with fine-scale techniques. Baltimore, MD: The Johns Hopkins University Press.

Crowder C, Rosella L. 2007. Assessment of intra- and intercostal variation in rib histomorphometry: its impact on evidentiary examination. J Forensic Sci 52:271–276.

Crowder CM. 2005. Evaluating the use of quantitative bone histology to estimate adult age at death. PhD Thesis. Toronto: University of Toronto.

Currey JD. 1988. The effect of porosity and mineral content on the Young's modulus of elasticity of compact bone. J Biomech 21:131–139.

Currey JD. 2002. Safety factors and scaling effects in bones. In: Bones: structure and mechanics. Princeton: Princeton University Press. p 309–336.

Currey JD, Brear K, Zioupos P. 2004. Notch sensitivity of mammalian mineralized tissues in impact. Proc Biol Sci 271:517–522.

Curtis TA, Ashrafi SH, Weber DF. 1985. Canalicular communication in the cortices of human long bones. Anat Rec 212:336–344.

Dominguez VM, Crowder CM. 2012. The utility of osteon shape and circularity for differentiating human and nonhuman Haversian bone. Am J Phys Anthropol Suppl 54:133.

Donahue SW, Galley SA. 2006. Microdamage in bone: implications for fracture, repair, remodeling, and adaptation. Crit Rev Biomed Eng 34:215–271.

Donahue SW, Sharkey NA, Modanlou KA, Sequeira LN, Martin RB. 2000. Bone strain and microcracks at stress fracture sites in human metatarsals. Bone 27:827–833.

Ericksen MF. 1991. Histologic estimation of age at death using the anterior cortex of the femur. Am J Phys Anthropol 84:171–179.

Ferretti M, Muglia MA, Remaggi F, Canè V, Palumbo C. 1999. Histomorphometric study on the osteocyte lacuno-canalicular network in animals of different species. II. Parallel-fibered and lamellar bones. Ital J Anat Embryol 104:121–131.

Frost HM. 2003. Bone's mechanostat: a 2003 update. Anat Rec A Discov Mol Cell Evol Biol 275:1081–1101.

Gray SK, Weyland DR, McGee-Lawrence ME, Wojda SJ, Donahue SW. 2012. Black bears with longer disuse (hibernation) periods have lower femoral osteon population density and greater mineralization. In: 58th Annual Meeting of the Orthopaedic Research Society. Orthopaedic Research Society, Rosemont, IL, Vol. 37. p 377.

Haines RW, Mehta L, Mohiuddin A. 1983. Nutrition of interstitial lamellae of bone. Anat Anz 154:233–236.

Hall BK. 2005. Skeletal origins: somitic mesoderm. In: Bones and cartilage: developmental and evolutionary skeletal biology. San Diego: Elsevier Academic Press. p 217–229.

Ham AW. 1952. Some histophysiological problems peculiar to calcified tissues. J Bone Joint Surg Am 24:701–728.

Hammer Ø, Harper DAT, Ryan PD. 2001. PAST: paleontological statistics software package for education and data analysis. Palaeontol Electron 4:1–9.

Heaney RP. 2003. How does bone support calcium homeostasis? Bone 33:264–268.

Hiller LP, Stover SM, Gibson VA, Gibeling JC, Prater CS, Hazelwood SJ, Yeh OC, Martin RB. 2003. Osteon pullout in the equine third metacarpal bone: effects of *ex vivo* fatigue. J Orthop Res 21:481–488.

Hillman JR, Davis RW, Abdelbaki YZ. 1973. Cyclic bone remodeling in deer. Calcif Tissue Res 12:323–330.

Hofman MA. 1988. Allometric scaling in paleontology: a critical survey. Hum Evol 3:177–188.

Huang R, Zhi Q, Schmidt C, Wilting J, Brand-Saberi B, Christ B. 2000. Sclerotomal origin of the ribs. Development 127:527–532.

Hulsey BI, Klippel WE, Jantz LM. 2009. Metacarpal and metatarsal histology of humans and black bears. Proc Am Acad Forensic Sci 15:303.

Huxley JS, Tessier G. 1936. Terminology of relative growth. Nature 137:780–781.

Jepsen KJ, Centi A, Duarte GF, Galloway K, Goldman H, Hampson N, Lappe JM, Cullen DM, Greeves J, Izard R, Nindl BC, Kraemer WJ, Negus CH, Evans RK. 2011. Biological constraints that limit compensation of a common skeletal trait variant lead to inequivalence of tibial function among healthy young adults. *J Bone Miner Res* 26:2872–2885.

Jordanoglou J. 1969. Rib movement in health, kyphoscoliosis, and ankylosing spondylitis. Thorax 24:407–414.

Kerley ER. 1965. The microscopic determination of age in human bone. Am J Phys Anthropol 23:149–163.

Kerschnitzki M, Wagermaier W, Roschger P, Seto J, Shahar R, Duda GN, Mundlos S, Fratzl P. 2011. The organization of the osteocyte network mirrors the extracellular matrix orientation in bone. J Struct Biol 173:303–311.

Lieberman DE, Pearson OM, Polk JD, Demes B, Crompton AW. 2003. Optimization of bone growth and remodeling in response to loading in tapered mammalian limbs. J Exp Biol 206:3125–3138.

Marotti G, Zallone AZ. 1980. Changes in the vascular network during the formation of Haversian systems. Acta Anat 106:84–100.

Martin R, Burr D, Sharkey N. 1998. Mechanical properties of bone. In: Skeletal tissue mechanics. New York: Springer-Verlag. p 127–180.

Martin RB. 2000. Does osteocyte formation cause the nonlinear refilling of osteons. Bone 26:71–78.

Martin RB. 2003. Fatigue damage, remodeling, and the minimization of skeletal weight. J Theor Biol 220:271–276.

Martin RB, Boardman DL. 1993. The effects of collagen fiber orientation, porosity, density, and mineralization on bovine cortical bone bending properties. J Biomech 26:1047–1054.

Mason MW, Skedros JG, Bloebaum RD. 1995. Evidence of strain-mode-related cortical adaptation in the diaphysis of the horse radius. Bone 17:229–237.

Metz LN, Martin RB, Turner AS. 2003. Histomorphometric analysis of the effects of osteocyte density on osteonal morphology and remodeling. Bone 33:753–759.

Mishra S, Knothe Tate ML. 2003. Effect of lacunocanalicular architecture on hydraulic conductance in bone tissue: implications for bone health and evolution. Anat Rec A Discov Mol Cell Evol Biol 273:752–762.

Morris ZH. 2007. Quantitative and spatial analysis of the microscopic bone structures of deer (*Odocoileus virginianus*), dog (*Canis familiaris*), and pig (*Sus scrofa domesticus*). Master's Thesis. Louisiana: Louisiana State University.

Mulhern DM. 2000. Rib remodeling dynamics in a skeletal population from Kulubnarti, Nubia. Am J Phys Anthropol 111:519–530.

Mulhern DM, Ubelaker DH. 2012. Differentiating human from nonhuman bone microstructure. In: Crowder C, Stout S, editors. Bone histology: an anthropological perspective. Boca Raton: CRC Press. p 109–134.

Okada S, Yoshida S, Ashrafi SH, Schraufnagel DE. 2002. The canalicular structure of compact bone in the rat at different ages. Microsc Microanal 8:104–115.

Ott SM, Lipkin EW, Newell-Morris L. 1999. Bone physiology during pregnancy and lactation in young macaques. J Bone Miner Res 14:1779–1788.

Palumbo C, Ferretti M, Marotti G. 2004. Osteocyte dendrogenesis in static and dynamic bone formation: an ultrastructural study. Anat Rec 278A:474–480.

Parfitt AM. 1983. The physiologic and clinical significance of bone histomorphometric data. In: Recker RR, editor. Bone histomorphometry: techniques and interpretation. Boca Raton: CRC Press. p 143–224. Chapter 9.

Parfitt AM. 1987. Bone and plasma calcium homeostasis. Bone 8(Suppl 1):S1–S8.

Parfitt AM. 1993. Calcium homeostasis. In: Mundy GR, Martin TJ, editors. Physiology and pharmacology of bone. Berlin: Springer-Verlag. p 1–65.

Parfitt AM. 2010. Skeletal heterogeneity and the purposes of bone remodeling: implications for the understanding of osteoporosis. In: Marcus R, Feldman D, Nelson DA, Rosen CJ, editors. Fundamentals of osteoporosis. San Diego: Academic Press. p 35–54.

Parfitt AM, Drezner MK, Glorieux FH, Kanis JA, Malluche H, Meunier PJ, Ott SM, Recker RR. 1987. Bone histomorphometry: standardization of nomenclature, symbols, and units.

Report of the ASBMR Histomorphometry Nomenclature Committee. J Bone Miner Res 2:595–610.
Pfeiffer S, Crowder C, Harrington L, Brown M. 2006. Secondary osteons and haversian canal dimensions as behavioral indicators. Am J Phys Anthropol 131:460–468.
Plotnick RE. 1989. Application of bootstrap methods to reduce major axis line fitting. Syst Zool 38:144–153.
Power J, Doube M, van Bezooijen RL, Loveridge N, Reeve J. 2012. Osteocyte recruitment declines as the osteon fills in: interacting effects of osteocytic sclerostin and previous hip fracture on the size of cortical canals in the femoral neck. Bone 50:1107–1114.
Qin L, Mak AT, Cheng CW, Hung LK, Chan KM. 1999. Histomorphological study on pattern of fluid movement in cortical bone in goats. Anat Rec 255:380–387.
Qing H, Ardeshirpour L, Pajevic PD, Dusevich V, Jahn K, Kato S, Wysolmerski J, Bonewald LF. 2012. Demonstration of osteocytic perilacunar/canalicular remodeling in mice during lactation. J Bone Miner Res 27:1018–1029.
Qiu S, Fyhrie DP, Palnitkar S, Rao DS. 2003. Histomorphometric assessment of Haversian canal and osteocyte lacunae in different-sized osteons in human rib. Anat Rec 272A:520–525.
Qiu S, Rao DS, Palnitkar S, Parfitt AM. 2002. Relationship between osteocyte density and bone formation rate in human cancellous bone. Bone 31:709–711.
Qiu S, Rao DS, Palnitkar S, Parfitt AM. 2010. Dependence of bone yield (volume of bone formed per unit of cement surface area) on resorption cavity size during osteonal remodeling in human rib: implications for osteoblast function and the pathogenesis of age-related bone loss. J Bone Miner Res 25:423–430.
Raab DM, Crenshaw TD, Kimmel DB, Smith EL. 1991. A histomorphometric study of cortical bone activity during increased weight-bearing exercise. J Bone Miner Res 6:741–749.
Rawlinson SD, Mosley JR, Suswillo RF, Pitsillides AA, Lanyon LE. 1995. Calvarial and limb bone cells in organ and monolayer culture do not show the same early response to dynamic mechanical strains. J Bone Miner Res 10:1225–1232.
Robling AG, Stout SD. 2003. Histomorphology, geometry, and mechanical loading in past populations. In: Agarwal SC, Stout SD, editors. Bone loss and osteoporosis: an anthropological perspective. New York: Kluwer Academic/Plenum Publishers. p 189–205.
Schilling N. 2011. Evolution of the axial system in craniates: morphology and function of the perivertebral musculature. Front Zool 8:4.
Schmidt-Nielsen K. 1984. Scaling: why is animal size so important? New York: Press Syndicate of the University of Cambridge.
Seim E, Saether B. 1983. On rethinking allometry: which regression model to use? J Theor Biol 104:161–168.
Shearman RM, Burke AC. 2009. The lateral somitic frontier in ontogeny and phylogeny. J Exp Zool B Mol Dev Evol 312:603–612.
Simons RS. 1999. Running, breathing and visceral motion in the domestic rabbit (*Oryctolagus cuniculus*): testing visceral displacement hypotheses. J Exp Biol 202:563–577.
Skedros JG. 2012. Interpreting load history in limb-bone diaphyses: important considerations and their biomechanical foundations. In: Crowder C, Stout S, editors. Bone histology: an anthropological perspective. Boca Raton: CRC Press. p 153–220.
Skedros JG, Clark GC, Sorenson SM, Taylor KW, Qiu S. 2011a. Analysis of the effect of osteon diameter on the potential relationship of osteocyte lacuna density and osteon wall thickness. Anat Rec 294:1472–1485.
Skedros JG, Holmes JL, Vajda EG, Bloebaum RD. 2005. Cement lines of secondary osteons in human bone are not mineral-deficient: new data in a historical perspective. Anat Rec A Discov Mol Cell Evol Biol 286:781–803.
Skedros JG, Hunt KJ, Bloebaum RD. 2004. Relationships of loading history and structural and material characteristics of bone: development of the mule deer calcaneus. J Morphol 259:281–307.
Skedros JG, Keenan KE, Halley JA, Knight AN, Bloebaum RD. 2012. Osteon morphotypes and predominant collagen fiber orientation are adaptations for habitual medial-lateral bending in the human proximal diaphysis: implications for understanding the etiology of atypical fractures. In: 58th Annual Meeting of the Orthopaedic Research Society. Orthopaedic Research Society: Rosemont, Illinois, Vol. 37; p 1512.
Skedros JG, Keenan KE, Williams TJ, Kiser CJ. 2013. Secondary osteon size and collagen/lamellar organization ("osteon morphotypes") are not coupled, but potentially adapt independently for local strain mode or magnitude. J Struct Biol 181:95–107.
Skedros JG, Kiser CJ, Keenan KE, Thomas SC. 2011b. Analysis of osteon morphotype scoring schemes for interpreting load history: evaluation in the chimpanzee femur. J Anat 218:480–499.
Skedros JG, Mason MW, Bloebaum RD. 2001. Modeling and remodeling in a developing artiodactyl calcaneus: a model for evaluating Frost's mechanostat hypothesis and its corollaries. Anat Rec 263:167–185.
Skedros JG, Mendenhall SD, Kiser CJ, Winet H. 2009. Interpreting cortical bone adaptation and load history by quantifying osteon morphotypes in circularly polarized light images. Bone 44:392–403.
Skedros JG, Sorenson SM, Jenson NH. 2007. Are distributions of secondary osteon variants useful for interpreting load history in mammalian bones? Cells Tissues Organs 185:285–307.
Skedros JG, Su SC, Bloebaum RD. 1997. Biomechanical implications of mineral content and microstructural variations in cortical bone of horse, elk, and sheep calcanei. Anat Rec 249:297–316.
Skedros JG, Sybrowsky CL, Anderson WE, Chow F. 2011c. Relationships between *in vivo* microdamage and the remarkable regional material and strain heterogeneity of cortical bone of adult deer, elk, sheep and horse calcanei. J Anat 219:722–733.
Skedros JG, Sybrowsky CL, Parry TR, Bloebaum RD. 2003. Regional differences in cortical bone organization and microdamage prevalence in Rocky Mountain mule deer. Anat Rec 274:837–850.
Smith RJ. 2009. Use and misuse of the reduced major axis for line-fitting. Am J Phys Anthropol 140:476–486.
Staub JF, Tracqui P, Lausson S, Milhaud G, Perault-Staub AM. 1989. A physiologic view of in vivo calcium dynamics: the regulation of a non linear self organized system. Bone 10:77–86.
Su SC, Skedros JG, Bachus KN, Bloebaum RD. 1999. Loading conditions and cortical bone construction of an artiodactyl calcaneus. J Exp Biol 2002:3239–3254.
Swartz SM, and Biewener AA. 1992. Shape and scaling. In: Biewener AA, editor. Biomechanics—structures and systems: a practical approach. New York: Oxford University Press. p 21–43.
Talmage RV, Lester GE, Hirsch PF. 2000. Parathyroid hormone and plasma calcium control: an editorial. J Musculoskel Neuron Interact 1:121–126.
Tommerup LJ, Raab DM, Crenshaw TD, Smith EL. 1993. Does weight-bearing exercise affect non-weight-bearing bone? J Bone Miner Res 8:1053–1058.
Turner CH. 2002. Biomechanics of bone: determinants of skeletal fragility and bone quality. Osteoporos Int 13:97–104.
Vajda EG, Kneissel M, Muggenburg B, Miller SC. 1999. Increased intracortical bone remodeling during lactation in beagle dogs. Biol Reprod 61:1439–1444.
van Oers RF, Ruimerman R, van Rietbergen B, Hilbers PA, Huiskes R. 2008. Relating osteon diameter to strain. Bone 43:476–482.
Vatsa A, Breuls RG, Semeins CM, Salmon PL, Smit TH, Klein-Nulend J. 2008. Osteocyte morphology in fibula and calvaria—is there a role for mechanosensing? Bone 43:452–458.
Vittinghoff E, Gllidden DV, Shiboski SC, McCulloch CE. 2005. Regression methods in biostatistics: linear logistic, survival, and repeated measures models. New York: Springer.
Wang L, Cowin SC, Weinbaum S, Fritton SP. 2000. Modeling tracer transport in an osteon under cyclic loading. Ann Biomed Eng 28:1200–1209.
Wilson AK, Bhattacharyya MH, Miller S, Mani A, Sacco-Gibson N. 1998. Ovariectomy-induced changes in aged beagles: histomorphometry of rib cortical bone. Calcif Tissue Int 62:237–243.
Zedda M, Lepore G, Manca P, Chisu V, Farina V. 2008. Comparative bone histology of adult horses (*Equus caballus*) and cows (*Bos taurus*). Anat Histol Embryol 37:442–445.